SECOND GENERATION ADVANCED REBURNING FOR HIGH EFFICIENCY NO_x CONTROL

Quarterly Report No. 13 for Period

October 1 – December 31, 2000

Prepared by:

Vladimir M. Zamansky, Pete M. Maly and Vitali V. Lissianski

January 29, 2001

DOE Contract No. DE-AC22-95PC95251

Submitted by:

GE Energy and Environmental Research Corporation

18 Mason, Irvine, CA 92618

Disclaimer

Abstract

This project is designed to develop a family of novel NO_x control technologies, called Second Generation Advanced Reburning (SGAR) which has the potential to achieve 90+% NO_x control in coal-fired boilers at a significantly lower cost than SCR. The thirteenth reporting period in Phase II (October 1 – December 31, 2000) included SGAR tests in which coal was used as the reburning fuel. All test work was conducted at GE-EER's 1.0 MMBtu/hr Boiler Simulator Facility. Three test series were performed including AR-Lean, AR-Rich, and reburning + SNCR. Tests demonstrated that over 90% NO_x reduction could be achieved with utilization of coal as a reburning fuel in SGAR. The most effective SGAR variant is reburning + SNCR followed by AR-Lean and AR-Rich.

Table of Contents

List of Figures

Figures **Page**

Executive Summary

This project is designed to develop a family of novel NO_x control technologies, called Second Generation Advanced Reburning (SGAR) which has the potential to achieve 90+% NO_x control in coal-fired boilers at a significantly lower cost than SCR. The thirteenth reporting period in Phase II (October 1 – December 31, 2000) included SGAR tests in which coal was used as the reburning fuel. All test work was conducted at GE-EER's 1.0 MMBtu/hr Boiler Simulator Facility. Two coals selected for these tests based on results of basic reburning studies were Consol Jones Fork and Knott-Floyd Land coals. Three test series were performed including AR-Lean, AR-Rich, and reburning+SNCR. For these tests natural gas was used as the primary fuel.

Tests demonstrated that over 90% NO_x reduction can be achieved with utilization of coal as a reburning fuel in SGAR. The most effective SGAR variant was reburning+SNCR followed by AR-Lean and AR-Rich. The same order of SGAR efficiencies was found in previous tests for firing natural gas as a reburning fuel. Tests showed that injection of promoters could significantly improve efficiency of SGAR.

Based on results of previous work, two papers (*Reburning Chemistry-Mixing Model* and *Effect of Metal-Containing Additives on NO_x Reduction in Combustion and Reburning*) have been prepared and submitted for the publication in *Combustion and Flame*. Copies of papers are attached.

Preparation of the Draft Final Report was in progress during the reporting period. The Report will be submitted to U.S. DOE during the next reporting period.

1.0 Introduction

This project is designed to develop a family of novel NO_x control technologies, called Second Generation Advanced Reburning (SGAR) which has the potential to achieve 90+% NO_x control in coal-fired boilers. The activities during the thirteenth reporting period in Phase II (October 1 – January 31, 2000) included SGAR tests in which coal was used as the reburning fuel. These tests were performed in conjunction with South Carolina Electric and Gas (SCE&G) that is considering installing basic coal reburning on multiple boilers with potential to subsequently utilize advanced coal reburning. Tests evaluating coal as a reburning fuel in basic reburning were reported in Quarterly Report No. 7 [1].

All test work was conducted at GE EER's 1.0 MMBtu/hr Boiler Simulator Facility (BSF) described in detail elsewhere [2]. Two coals selected for these tests, based on results of basic reburning studies [1], were Consol Jones Fork and Knott-Floyd Land coals. Three test series were performed including AR-Lean, AR-Rich, and reburning+SNCR. For these tests natural gas was used as the primary fuel. Initial NO_x concentration was 400 ppm. Reburning fuel was injected at 1700 K. In all tests SR_1 = 1.1 and SR_3 = 1.15 while SR_2 was a variable. Urea was injected at Nitrogen Stoichiometric Ratio N/NO = NSR = 1.5. The following sections describe results of advanced coal reburning studies.

2.0 AR-Lean with Coal Reburning

Figure 1 shows AR-Lean performance as a function of injection temperature for Consol Jones Fork and Knott-Floyd Land coals. Reburning heat input was 10%. With each coal performance increased with decreasing injection temperature. Maximum NO_x reductions were 57% for Knott-Floyd Land coal and 62% for Consol Jones Fork coal, both obtained at an injection temperature of 1310 K. These results represent an incremental improvement of 17-20 percentage points over basic reburning.

Figures 2 shows promoted AR-Lean performance as a function of flue gas sodium concentration for Consol Jones Fork and Knott-Floyd Land coals. Overfire air (OFA) was injected at 1310 K. With each coal sodium dramatically increased NO_x reduction. With Consol Jones Fork coal, NO_x reduction increased from 62% with no sodium to 90% with 150 ppm sodium. With Knott-Floyd Land coal under similar conditions NO_x reduction increased from 57 to 82%.

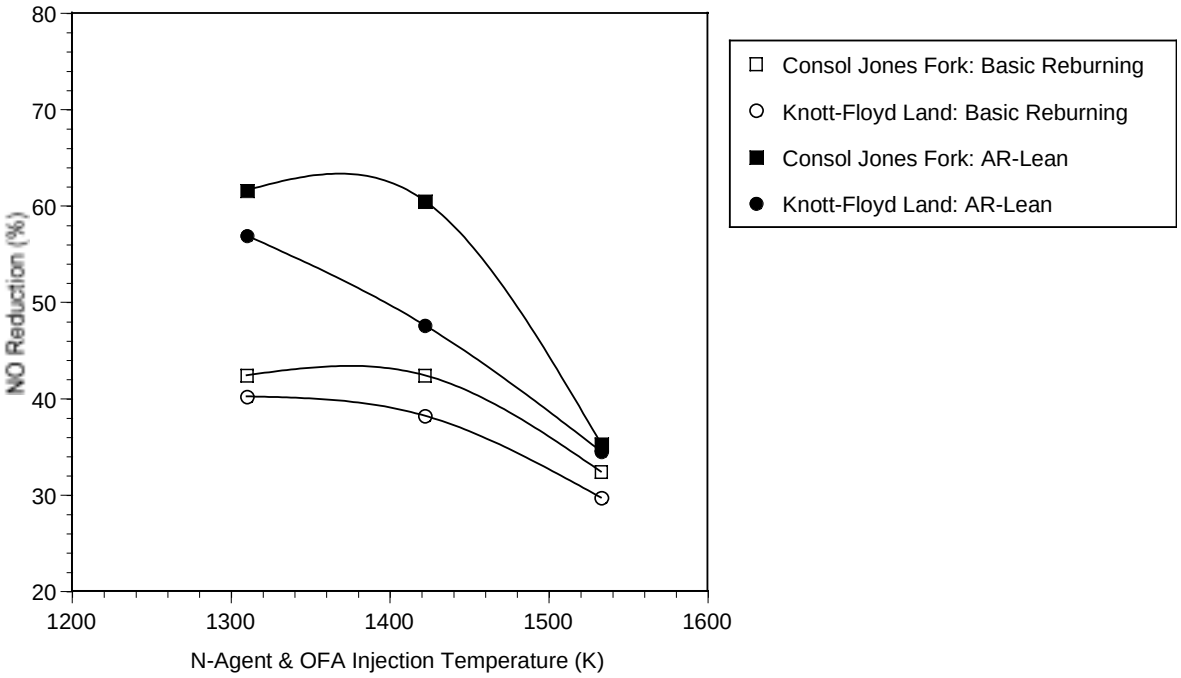

Figure 1. AR-Lean performance at 10% reburning as a function of N-agent/OFA injection temperature for Consol Jones Fork and Knott-Floyd Land coals.

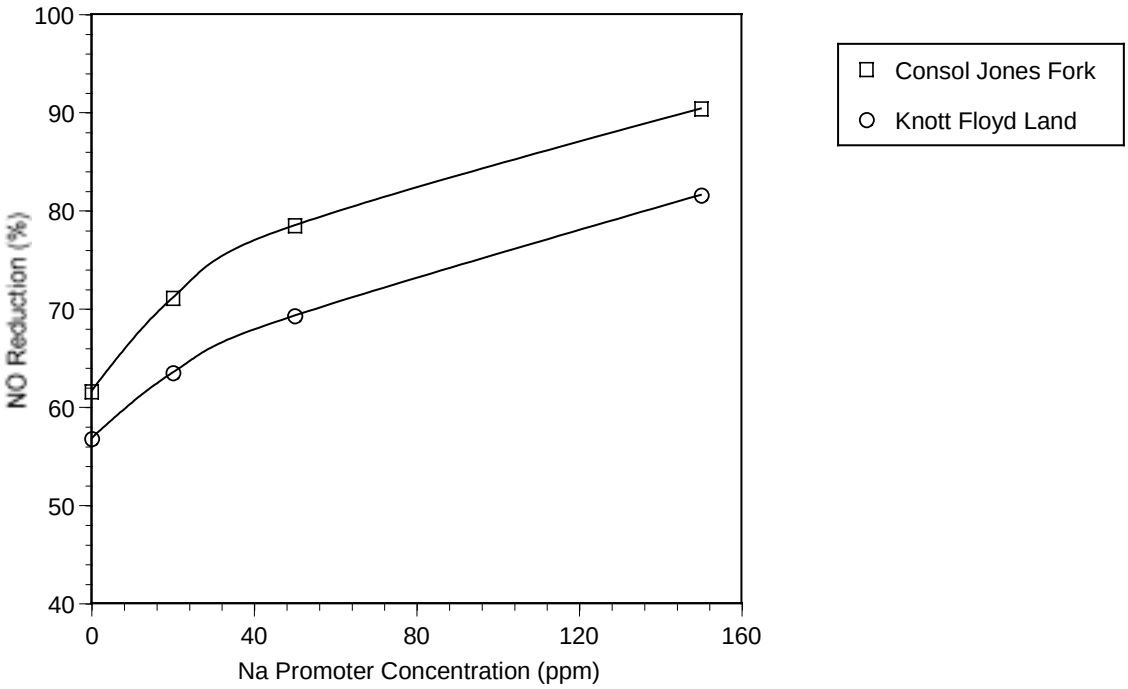

Figure 2. Promoted AR-Lean performance at 10% reburning as a function of promoter concentration for Consol Jones Fork and Knott-Floyd Land coals. Na_2CO_3 is co-injected with urea.

3.0 AR-Rich with Coal Reburning

Figure 3 shows AR-Rich performance as a function of N-agent injection temperature for Consol Jones Fork and Knott-Floyd Land coals. Urea was injected at 1310-1530 K and OFA was injected at 1300 K. Maximum NO_x reduction for Consol Jones Fork and Knott-Floyd Land coals was 58% and 61%, respectively, obtained at injection temperature of 1400 K. Figure 4 shows promoted AR-Rich performance as a function of flue gas sodium concentration. Adding 150 ppm sodium caused NO_x reduction to increase from 57% with no promoter to 65% with 150 ppm Na for Knott-Floyd Land coal and from 53% to 72% for Consol Jones Fork coal, which is a lower increase than that observed during AR-Lean tests.

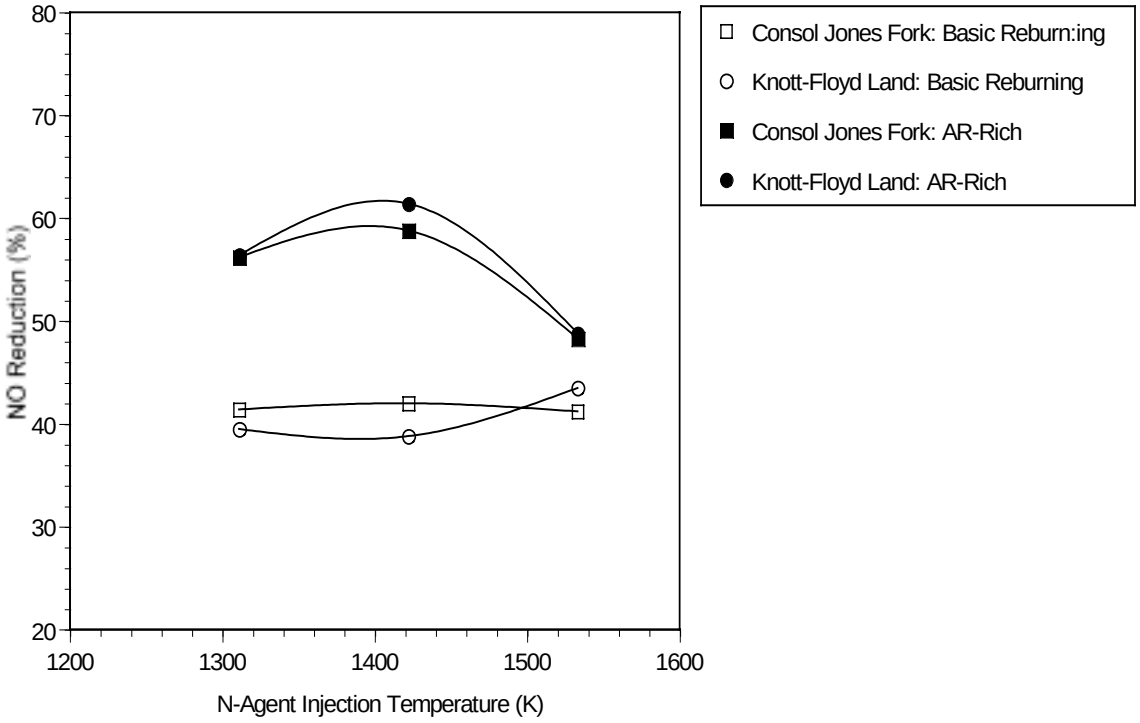

Figure 3. AR-Rich performance at 10% reburning as a function of N-agent injection temperature for Consol Jones Fork and Knott-Floyd Land coals.

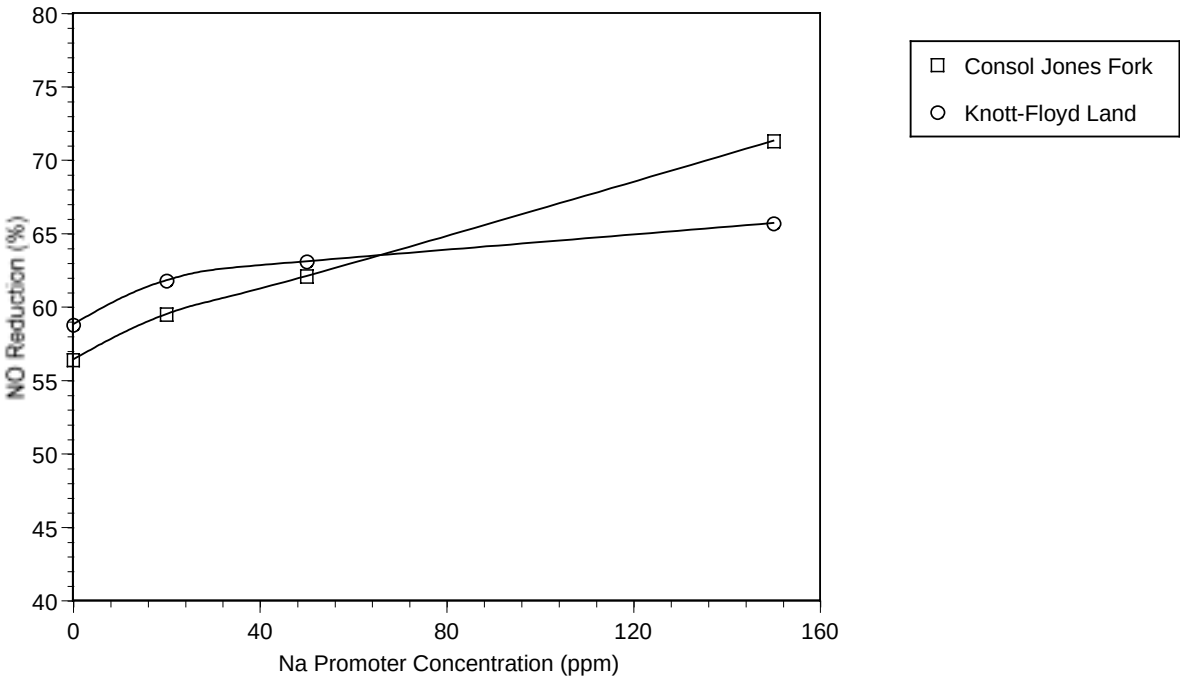

Figure 4. Promoted AR-Rich performance at 10% reburning as a function of promoter concentration for Consol Jones Fork and Knott-Floyd Land coals. Na_2CO_3 is co-injected with urea.

4.0 Coal Reburning + SNCR

Reburning+SNCR tests were conducted at various N-agent injection temperatures, reburning heat inputs, and sodium promoter concentrations. Figure 5 shows results as a function of N-agent injection temperature for Consol Jones Fork and Knott-Floyd Land coals. With each coal NO_x reduction increased with decreasing injection temperature. Maximum NO_x reduction for both coals was about 90%, achieved at an injection temperature of 1230 K.

Figure 6 shows reburning+SNCR results as a function of reburning heat input. OFA was injected at 1530 K, urea at 1200 K. With each coal, overall NO_x reduction showed minimal dependence on reburning heat input. Better performance was achieved with Consol Jones Fork coal than Knott-Floyd Land coal.

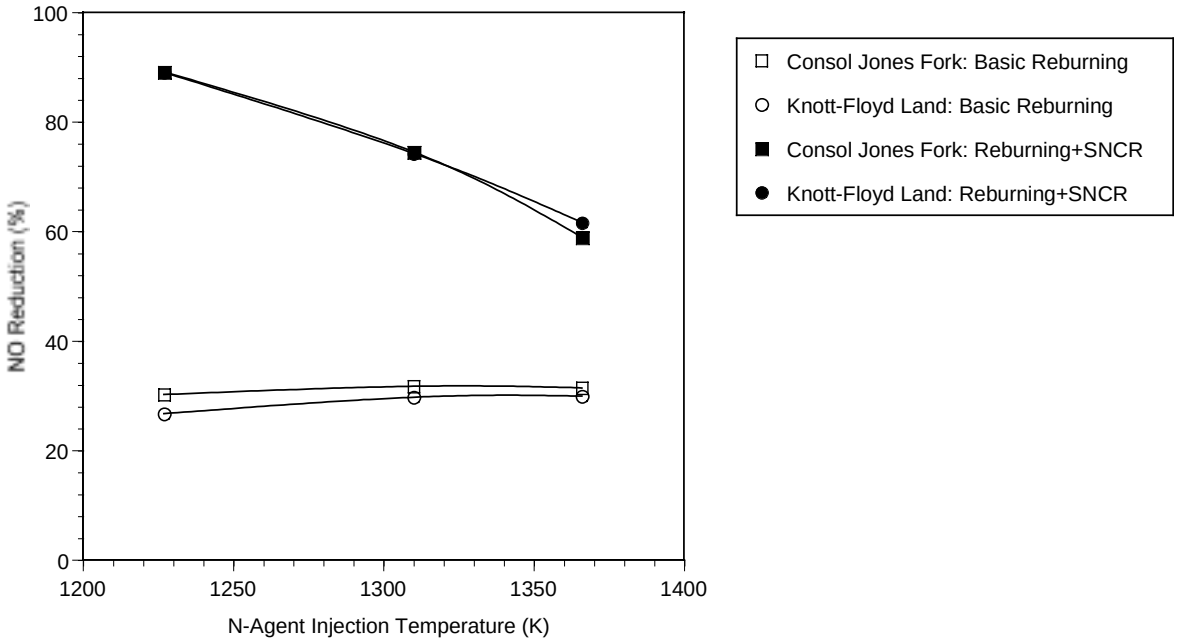

Figure 5. Combined reburning/SNCR performance at 10% reburning as a function of N-agent injection temperature for Consol Jones Fork and Knott-Floyd Land coals.

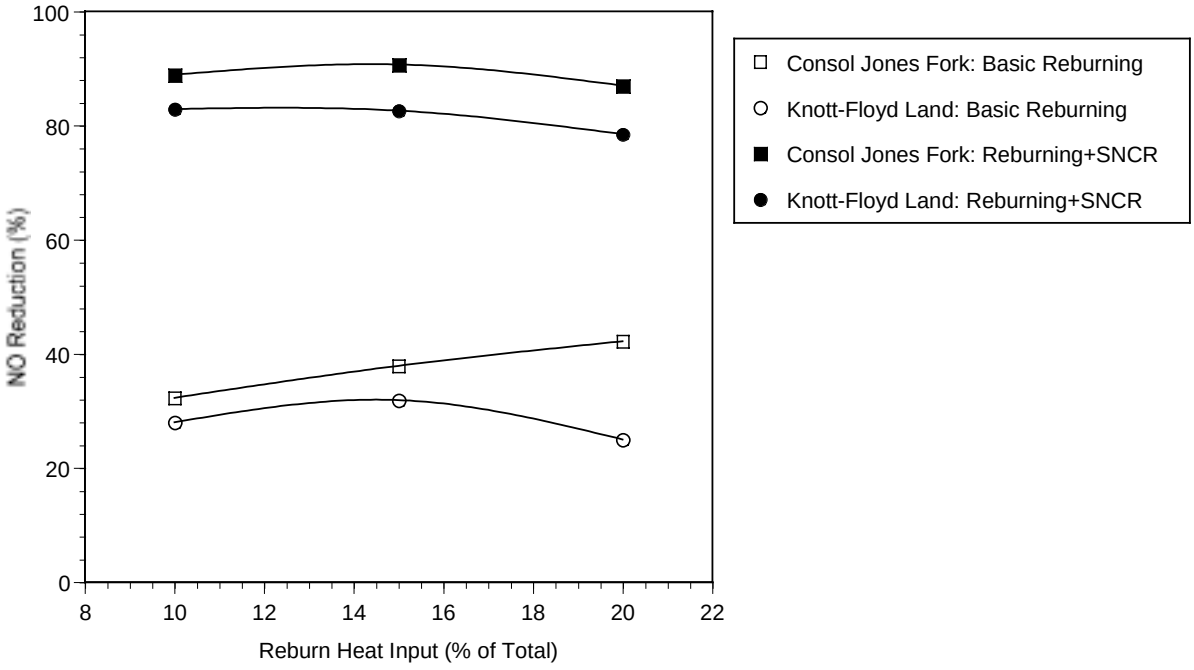

Figure 6. Combined reburning/SNCR performance as a function of reburning heat input for Consol Jones Fork and Knott-Floyd Land coals.

Figure 7 shows reburning+SNCR results as a function of sodium promoter concentration. The sodium was co-injected with the N-agent at 1230 K. In each case the sodium had minimal effect on performance, likely because the injection temperature was too low.

The final series of tests involved promoted reburning with no N-agent. The promoter consisted of an iron oxide waste material that was co-injected with the reburning coal. Iron concentration in the flue gas was varied from 0 to 1,000 ppm. Figure 8 shows NO_x reduction as a function of Fe promoter concentration for Consol Jones Fork and Knott-Floyd Land coals. Greater promotion was obtained with the Knott-Floyd Land coal, for which NO_x reduction increased from 36% to 46% as Fe increased from 0 to 1,000 ppm.

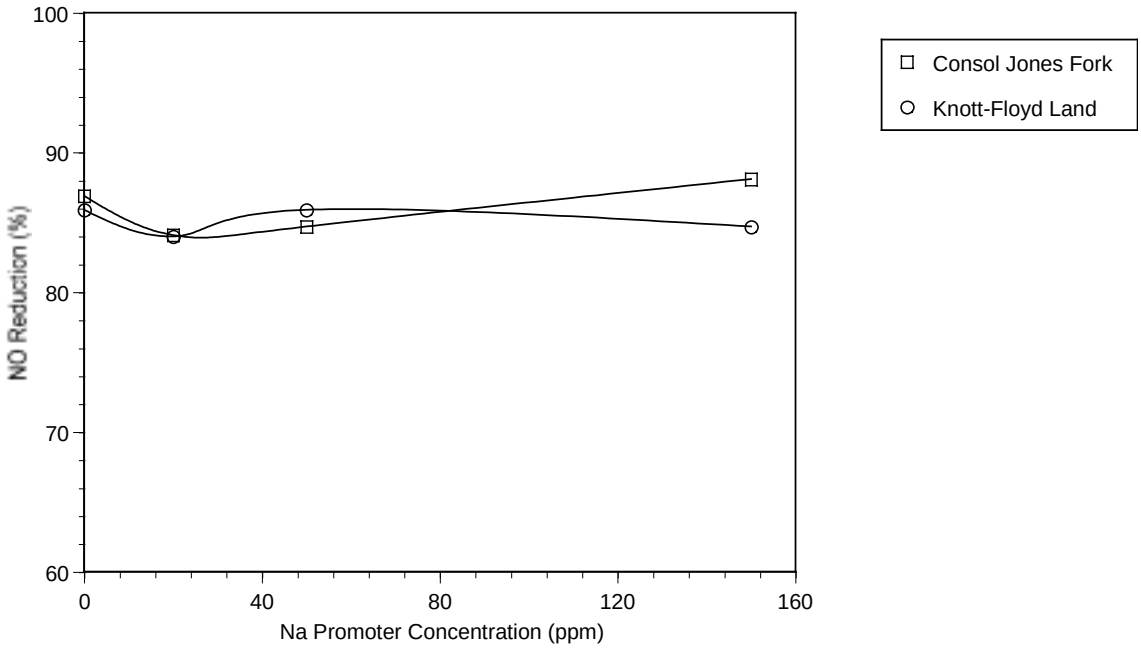

Figure 7. Combined reburning/SNCR performance at 15% reburning as a function of promoter concentration for Consol Jones Fork and Knott-Floyd Land coals.

5.0 Advanced Coal Reburning: Summary

The following conclusions can be drawn from test data:

1. Over 90% NO_x reduction can be achieved with utilization of coal as a reburning fuel in SGAR.
2. The most effective SGAR variant is reburning+SNCR followed by AR-Lean and AR-Rich. The same order of SGAR efficiencies was found for firing natural gas as a reburning fuel. Tests showed that injection of promoters could significantly improve the efficiency of SGAR.

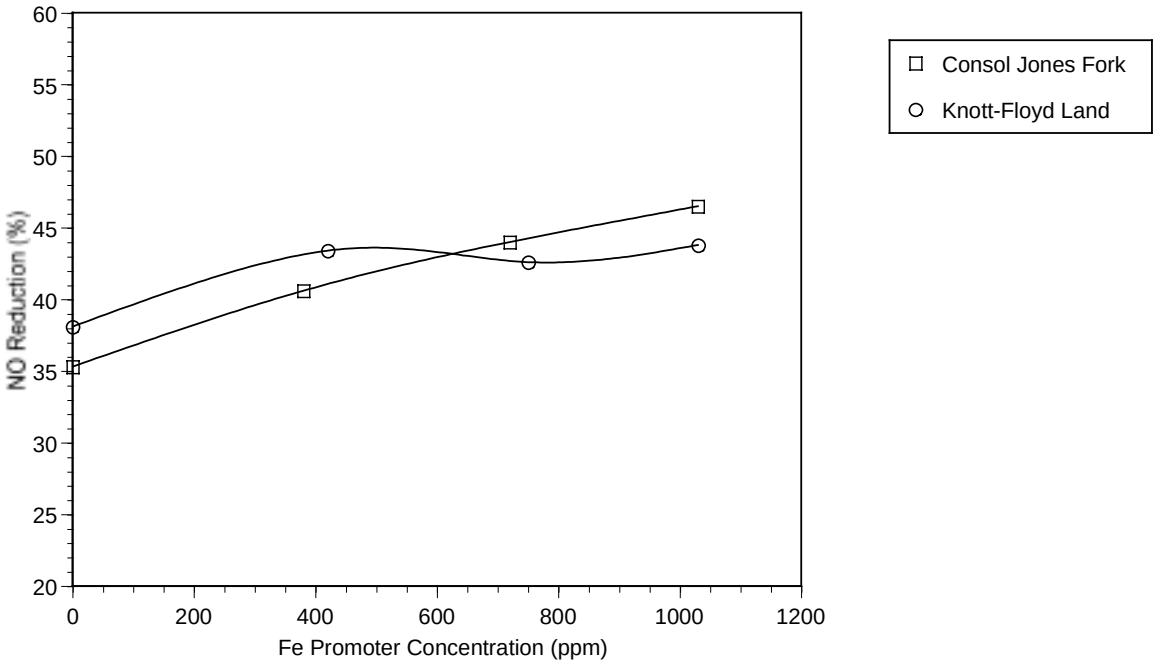

Figure 8. Effect of Fe promoter concentration on reburning. The amount of the reburning fuel is 15%.

6.0 Future Work

Future activities will include preparation of Final Report. It is anticipated that Final Report will be submitted to U.S. DOE in April, 2001.

7.0 Bibliography

1. Zamansky, V.M., Maly, P.M., and Lissianski, V.V. (1999) Second Generation Advanced Reburning for High Efficiency NO_x Control. *Quarterly Report No. 7, DOE Contract No. DE-AC22-95PC95251.*
2. Zamansky, V.M., Maly, P.M., and Lissianski, V.V. (1999) Second Generation Advanced Reburning for High Efficiency NO_x Control. *Quarterly Report No. 6, DOE Contract No. DE-AC22-95PC95251.*

Attachment A

Reburning Chemistry-Mixing Model

Vitali V. Lissianski, Vladimir M. Zamansky and Mark S. Sheldon

GE Energy and Environmental Research Corporation

18 Mason, Irvine, CA 92618

Full-length paper

Corresponding author:

Vitali Lissianski

GE Energy and Environmental Research Corporation, 18 Mason, Irvine, CA 92618

Phone: (949) 859-8851

Fax: (949) 859-3194

E-mail: vitali.lissianski@ps.ge.com

Reburning Chemistry-Mixing Model

Abstract

It is recognized that mixing has a significant impact on the performance of reburning. Realistic description of the reburning fuel distribution within the mixing area is an important part of a predictive model of the reburning process. Current approaches to represent mixing range in complexity from distributed addition of reagents to 3-dimensional computational fluid dynamics modeling. This work demonstrates that an approach combining a detailed description of the reburning chemistry with a distributed addition of reagents in the mixing area can be used to describe main features of the reburning process. The important feature of the model is the utilization of inverse mixing. The model is validated against experimental data obtained in five combustion facilities ranging in scale from bench- to large pilot-scale.

Reburning Chemistry-Mixing Model

Vitali V. Lissianski, Vladimir M. Zamansky and Mark S. Sheldon

GE Energy and Environmental Research Corporation

18 Mason, Irvine, CA 92618

Introduction

Reburning is a commercial technology which removes NO_x from combustion products using fuel as the reducing agent. The efficiency of NO_x removal depends on many factors primarily the type and the amount of the reburning fuel, locations where reburning fuel and overfire air (OFA) are injected, and intensity of mixing in the reburning zone. These parameters can be optimized for the highest NO_x reduction if a descriptive model of reburning is available.

Coupling of chemical kinetics and gas dynamics is recognized [1-15] to be important for modeling of the reburning process. For the last several years the predominant approach for representation of mixing in reburning modeling has changed from utilization of instantaneous mixing of reagents in the reburning zone [1,2] to incorporation of the mixing process in a simplified form [3-13] and inclusion of a 3-dimensional description of mixing [14-16]. The Local Integral Moment (LIM) approach [16] that combines 3-dimensional mixing with detailed chemistry is already available for modeling of practical combustion systems. However, due to computer limitations most currently available computational fluid dynamics (CFD) codes can be used only with simplified chemistry. Thus, simplifications in representation of the mixing process or reaction chemistry are required for the model to be executed within a reasonable computational time.

The chemistry of the reburning process can be reduced to several steps and combined with a 3-dimensional description of the mixing process. While many questions on details persist

[17,18], there is basic agreement about the main features of the reburning mechanism. However, reduction of combustion mechanisms is possible when the detailed mechanism is known. For example, utilization of additives to improve the efficiency of reburning and advanced reburning (a combination of reburning and injection of nitrogen-containing additives) [19,20] required use of detailed combustion chemistry to understand how additives affect NO_x reduction. In those studies, injection of nitrogen-containing additives (N-agents) and promoters (organic and inorganic salts of some metals) into the reburning zone resulted in 95% NO_x reduction. Once the pathways by which additives affect N-chemistry are understood, the kinetic mechanism can be developed, then simplified and combined with CFD modeling.

An alternative to the simplification of the combustion chemistry is simplification of the mixing process. The level of simplification in mixing modeling depends on the complexity of the mixing process, which, to some degree, depends on the scale of the combustion facility under investigation. Due to the fast mixing and relatively uniform temperature distribution in the reaction area, experiments in lab-scale facilities can be usually described using a one-dimensional representation of mixing. This approach is often applied to the description of reburning in bench- and pilot-scale facilities, but is not appropriate for the description of tests in full-scale combustion facilities.

Cha et al. [3] and *Han et al.* [4] demonstrated that the effect of finite-mixing on the reburning performance could be described using the Two-Stage Lagrangian model. Simple distributed addition of reagents was also found [5-13] in many cases to give good agreement with experimental data. The success of that approach can be attributed to the fact that despite its simplicity, it accounts for segregation of reactants in the mixing area of the reburning zone. The advantages of the approach are its simplicity and its suitability for implementation using widely used kinetic codes such as Chemkin-II [21].

The motivation for this work is to demonstrate that the reburning chemistry-mixing model (RCMM) [5] based on distributed addition of reactants in the mixing area can be used to predict the performance of reburning in bench- and pilot-scale combustion facilities. Such a model can be used not only for optimization of reburning, but can also be applied to advanced reburning to identify most important parameters affecting NO_x reduction. Validation of such a model also validates detailed kinetic mechanism which later can be used to derive reduced mechanisms used in CFD modeling of reburning and advanced reburning.

The feature that distinguishes RCMM from many other models of distributed addition of reagents is the utilization of the inverse mixing approach. The RCMM utilizes plug flow reactors to describe processes that occur in the boiler: mixing of the reburning fuel with flue gas, NO_x reduction in the reburning zone, addition of OFA, and reactions in the burnout zone. The mixing is described by using Zweietering approach [22] (the secondary stream is distributed along the primary stream in a continuous fashion over a certain period of time).

This paper presents validation of the RCMM over a wide range of mixing conditions and describes application of the model to the description of reburning in several combustion facilities ranging from bench- to large pilot-scale. Modeling predictions are compared with experimental data obtained in this work as well as with literature data.

Experimental

Experimental data used for comparison with modeling predictions were obtained in three combustion facilities: 20 kW Controlled Temperature Tower (CTT), 300 kW Boiler Simulator Facility (BSF), and 3 MW Tower Furnace (TF), which were described in more detail elsewhere [23,24]. Data of *Kolb et al.* [25] and *Mereb and Wendt* [26,27] were also used for model validation.

As shown in Figure 1a, the CTT is a vertically downfired combustor. It has a nominal firing rate of 20 kW. The furnace has an inside diameter of 20 cm and a length of 3 m. Furnace walls consist of layers of high temperature castable refractory. The furnace is equipped with numerous axial ports to allow introduction of additive injectors and sample probes. The quarl stabilizes the flame in the center of the furnace. The CTT is equipped with a variable swirl diffusion burner that is capable of firing coal, oil, or natural gas. Burner swirl number can be varied to control flame characteristics.

The BSF (Fig. 1b) is designed to provide an accurate sub-scale simulation of the flue gas temperatures and composition found in full-scale boiler. The BSF consists of a burner, vertically down-fired radiant furnace, and horizontal convective pass. Numerous ports located along the axis of the facility allow supplementary equipment such as additive injectors and sampling probes to be placed in the furnace. The cylindrical furnace has an inside diameter of 55 cm and a height of 7 m. It is constructed of eight modular refractory-lined sections. Heat extraction in the radiant furnace and convective pass is controlled so that the residence time-temperature profile matches that of a typical full-scale burner. A suction pyrometer is used to measure furnace temperature.

The TF (Fig. 1c) is a down-fired pilot plant combustor designed to provide a large-scale simulation of the flame properties, temperatures, gas compositions, and characteristic mixing times of a coal-fired boiler. As shown in Fig. 1c, the TF consists of a burner section, radiant furnace, convective pass, and set of air pollution control devices. The furnace is a refractory lined, water-cooled steel shell. It is square, having dimensions of 1.2 m across and 9 m in height. It has numerous axial ports, allowing access for injectors and sample probes. The transition between the furnace and convective pass is a nose section, having geometry and gas flow field characteristics similar to those of a coal fired boiler.

The process performance in the CTT, BSF and TF was characterized by continuous emissions monitors, consisting of a water-cooled sample probe, sample conditioning system (to remove water and particulate), and gas analyzers. It provided an online analysis of O_2, NO_x, CO, and CO_2 in flue gas. The uncertainty of experimental measurements was estimated to be ±5%.

In all tests natural gas was used as both primary and reburning fuel. Temperatures of flue gas at the point of the reburning fuel and OFA injection and the initial NO_x concentrations $[NO_x]_i$ are presented in Table 1. Axial temperature profiles measured in CTT, BSF and TF are presented in Figure 2.

In all tests, the stoichiometric ratio SR_1 for the primary combustion zone was 1.1. The amount of the reburning fuel varied from 5-25% of the total amount of fuel for the reburning zone stoichiometric ratio SR_2 of 0.83 – 1.05. The mixture composition in the burnout zone (including previously added fuel) corresponded to SR_3 = 1.15. Adding a controllable amount of NH_3 to the primary fuel regulated the initial NO_x concentration in the primary zone.

Modeling

Model Setup

Model setup is described in this section only briefly. Details of the model are presented in reference [5]. The following are highlights of the modeling approach.

- The model utilizes one-dimensional plug flow reactors to describe processes that occur in the boiler: mixing of the reburning fuel with flue gas, NO_x reduction in the reburning zone, addition of OFA, and reactions in the burnout zone.
- Mixing of the reburning fuel and OFA with flue gas occurs over a certain period of time (mixing time).

- The mixing process in the reburning zone is described by addition of flue gas to the stream of natural gas during a specified mixing time (so-called inverse mixing as distinguished from adding fuel to flue gas). Inverse mixing is also used to describe injection of OFA into flue gas.
- The composition of products, except for NO_x, exiting primary combustion zone is assumed to correspond to equilibrium conditions at the experimental values of temperature.
- The kinetic mechanism [28] includes 447 reactions of 65 C-H-O-N chemical species.
- The chemical kinetic code ODF (for "One Dimensional Flame") [29], was employed to execute model calculations for comparison with experimental data.

Description of the mixing approach in the model requires additional attention. As was noted in *Introduction*, several models have been developed using distributed addition of reagents to describe mixing in the reburning area. The distinguishing feature of the current approach is utilization of inverse mixing in conjunction with distributed addition. An example configuration describing application of this approach to represent mixing in the reburning zone is sketched in Fig. 3.

In the inverse mixing approach, the stream of reburning fuel is the main stream while flue gas exiting from the main combustion zone is added to it. As a result, the temperature history in the mixing area is described relative to the reburning stream rather than to the stream of flue gas. Thus, temperature in the mixing area at time $t = 0$ corresponds to the initial temperature of the reburning fuel. As mixing progresses, temperature increases until it reaches the temperature of flue gas. After reburning fuel and flue gas are completely mixed, there is no difference in their temperatures.

Mixing time in the reburning zone depends on several factors including configuration of the reburning fuel injection, velocities and temperatures of the reburning fuel and flue gas

streams, compositions of each stream, etc. The temperature profile presented in Fig. 3 is calculated for parameters of the reburning fuel injection used in BSF for the temperature of flue gas of 1670 K and initial temperature of the reburning fuel of 300 K. The mixing time determined from this profile is about 120 ms. Thus, modeling setup in the reburning zone of BSF includes two plug-flow reactors: the first reactor has residence time of 120 ms and describes mixing of the reburning fuel and flue gas using inverse mixing approach, the second reactor has residence time of 700 ms and describes the remainder of the reburning zone. The residence time in the second plug-flow reactor is determined by flue gas temperatures at which reburning fuel and OFA are injected, and temperature gradient in the BSF. The same approach was used to describe mixing of OFA and flue gas.

A similar approach was used for RCMM setup for CTT and TF.

The following parameters are inputs for RCMM:

- The relative amount of reburning fuel, OFA, and primary flue gas.
- The mean axial temperature gradient in the combustor.
- Temperatures of the flue gas at the point where reburning fuel and OFA are injected.
- Initial temperatures of the reburning fuel and OFA.
- Initial NO_x concentration in the primary zone.
- Mixing times in the reburning and burnout zones.
- Temperature profiles in mixing areas.

Mixing times and temperature profiles in mixing areas were determined for each combustion facility. The following sub-section describes approaches employed to determine these parameters.

Mixing Parameters

Mixing times and temperature profiles in mixing regions of CTT and BSF were calculated using a single-jet-in-cross-flow model [30]. A two-dimensional model was used based on previous experience suggesting relatively homogeneous distributions of temperature and mixture composition along cross sections of these combustors. Since TF is a much larger facility and is characterized by less uniform temperature and concentration fields across the furnace, mixing parameters in TF were estimated by CFD modeling with the commercial FLUENT software [31].

The single jet model JICFIS [30] determines mixing by evaluating the entrainment rate of fluid from the cross flow (in this case, the furnace gas) into the jet. The model is based on a simplified two-dimensional representation of the fluid dynamic equations for the jet. Major inputs for the model include the velocity and density ratios of the cross flow to the jet, their relative orientation in two dimensional rectangular coordinates, and the initial conditions (diameter, velocity, and temperature) of the jet.

A three-dimensional CFD model of the upper furnace and convective pass portion of TF was set in FLUENT [31] to simulate mixing in the reburning and burnout zones. The temperature profile was calibrated to measurements at specific points in the TF (Fig. 2). Velocity profiles at the inlet reburning and overfire planes were obtained from physical flow modeling measurements. Once the temperature and convective pass pressure drop were calibrated in the model, reburning fuel and OFA were injected through appropriate ports. From these results, mixing times in the reburning and burnout zones were determined.

Table 2 presents calculated mixing parameters for CTT, BSF and TF. The effect of mixing time on modeling predictions is discussed in the following section.

Results

This section describes validation of RCMM over wide ranges of process conditions. Previous work [5] demonstrated that RCMM predicted the main trends of the reburning process observed in the 300 kW BSF combustor. The model correctly described NO_x reduction efficiencies determined in experiments as functions of the initial NO_x concentration, the amount of reburning fuel and the OFA injection temperature. Modeling demonstrated that the most important parameters affecting the efficiency of the reburning process included (1) the amount of reburning fuel, (2) the initial NO_x level, (3) the initial temperatures of the injected reburning fuel and OFA, (4) the temperatures of flue gas at the points where reburning fuel and OFA are injected, (5) the mixing time of reburning fuel and OFA jets with flue gas, and (6) the intensity of mixing of the reburning fuel and OFA with flue gas.

Data presented here validate the RCMM and demonstrate that the model can be applied to describe basic reburning in different combustion facilities if their mixing and thermal characteristics are available. Modeling predictions are compared with experimental data obtained in this work as well as with literature data.

Comparison with Experimental Data in CTT, BSF and TF

Figure 4 shows comparison of modeling predictions with experimental data obtained in the CTT, BSF and TF. The RCMM correctly describes the reburning efficiency at different amounts of the reburning fuel and $[NO_x]_i$, and thus can correctly predict trends in NO_x reduction via reburning in combustion facilities ranging in scale from 20 kW to 3 MW.

Modeling results presented in Fig. 4 were obtained using values of mixing times from Table 2. Since two-dimensional models (for example, single-jet-in-cross-flow) do not precisely match experimental configurations for the reburning fuel injection, a practical issue is to determine how accurate the calculation of the mixing time for the model should be to give a

reasonable agreement of modeling predictions with experimental data. Thus, it is important to determine sensitivity of modeling predictions to the value of the mixing time. Figure 5 shows the effect of mixing time in the reburning zone on modeling predictions for typical BSF conditions. Experimental value of NO_x reduction for these conditions is also shown. Although Figure 5 demonstrates that the effect of mixing time impacts predicted NO_x reduction over the entire range of tested times, it also shows that it is the most significant at small mixing times (the transition from instantaneous mixing to finite-rate distributed addition of reagents). As mixing time increases, the effect of mixing time on NO_x reduction levels off. Thus, variation of the mixing time within ±50% from the value adopted in modeling (120 ms) does not significantly change modeling predictions. This justifies the use of simple models for calculating mixing times. It should be remembered, however, that if mixing area is characterized by significant radial and axial temperature non-uniformities, a more sophisticated approach is needed to calculate mixing parameters.

Comparison with Experimental Data of Kolb et al. [25]

Modeling predictions were also compared with experimental data of *Kolb et al.* [25] who studied the effect of mixing on the reburning efficiency in a 350 kW combustor. The authors used methane doped with NH_3 as primary and reburning fuel. Variation in mixing time was achieved by changing jet momentum (adding nitrogen to the stream of the reburning fuel). In particular, experimental data are reported for two jet velocities which are referred by authors as the low and high momentum jets. Under tests conditions reported by *Kolb et al.* [25], *Rota et al.* [9] calculated characteristic mixing times of the low and high momentum jets to be 50 and 10 ms. Calculations [9] using a single-jet-in-cross-flow model also showed that the high velocity reburning fuel jet reached walls of the furnace before complete mixing with flue gas occurred. The 10 ms mixing time for this jet was taken as the time required for the jet to reach walls. Thus,

the “real” mixing time for the high velocity jet was probably longer than 10 ms. Since the actual configuration of the reburning fuel injection (twenty gas jets) does not precisely match the single jet, as specified by the single jet in cross flow model, these times are approximate and can be considered as order of magnitude estimate.

Figure 6 shows comparison of model-predicted and measured [25] NO_x reduction at the end of the reburning zone for low and high momentum jets. Initial $[NO_x]_i$ concentrations were 980 ppm for the high and 1,230 ppm for the low momentum jets. In modeling, mixing time was an adjustable parameter. For the low velocity jet, the best agreement with experimental data was achieved at 60 ms mixing time which is close to the estimate of 50 ms made by *Rota et al.* [9]. For high velocity jet, the best agreement was obtained at 40 ms mixing time which is longer than *Rota et al.* [9] estimate. However, since actual mixing time of the high velocity jet is probably longer than 10 ms, this result can be considered to be reasonable by comparison with the *Rota et al.* [9] estimate. Good agreement of modeling predictions with experimental data (Fig. 6) suggests that RCMM correctly describes main features of the reburning process observed by *Kolb et al.* [25].

Another observation regarding the effect of mixing on reburning can be derived from Fig. 6. Both experimental data and modeling predictions suggest that at low heat inputs of the reburning fuel (SR_2 in the range of 0.9-1.0) the process is more effective at longer mixing times (the low momentum jet), while at larger heat inputs ($SR_2 < 0.9$) better mixing (the high momentum jet) is more favorable. This finding supports modeling conclusion [5] that fast mixing of reactants improves NO_x reduction at large amounts of the reburning fuel, while significant mixture stratification and longer mixing times gives better NO_x control at small amounts of the reburning fuel.

Comparison with Experimental Data by Mereb and Wendt [26,27]

Mereb and Wendt [26,27] reported NO_x concentrations in the reburning zone of a laboratory combustor as function of SR_2. Temperatures of the flue gas at which reburning fuel was injected varied from 1380 to 1600 K. The reported mixing time was 0.18 s. The primary fuel was coal while the reburning fuel was natural gas. Since the reburning fuel was deliberately injected significantly downstream from the primary coal flame to allow sufficient time for char burnout, the nature of the primary fuel probably had a little or no effect on the reactions in the reburning zone.

Figure 7 compares measured [26] and predicted performances of the reburning process as a function of SR_2. Modeling was done for 0.18 s mixing time. Modeling predictions agree well with experimental data at SR_2 in the range of 0.9-1.15 and slightly overpredict the efficiency of the reburning process at $SR_2 < 0.9$. The measured maximum in the reburning efficiency at SR_2 about 0.9 is well matched by the model predictions.

Figure 8 shows a comparison of predicted and measured [26] NO_x concentration profiles in the reburning zone for $SR_2 = 0.68$ and 0.80 shown as a function from the time from reburning fuel injection. While some deviations between experimental data and modeling predictions can be seen at the beginning and in the middle of the reburning zone, the predicted NO_x concentrations at the end of the reburning zone for both cases are in a good agreement with experimental values. This agreement is encouraging since mixing time 0.18 s reported by *Mereb and Wendt* [26] was used in modeling and none of the RCMM parameters was adjusted to improve agreement with experimental data.

Conclusions

Two main factors determine success in the development of a model for the reburning process: a correct description of the reaction chemistry and realistic assumptions concerning reactant mixing. The motivation for this work was to demonstrate that the reburning model based

on detailed chemistry [28] and distributed addition of reactants in the mixing area can be used to describe reburning performance of the bench- and pilot-scale combustion facilities covering two orders of magnitude in firing rates. The distinguishing feature of the model is the utilization of inverse mixing. Modeling results correctly describe a wide range of experimental data obtained in five bench- and pilot-scale combustion facilities. This suggests that developed model represents the main chemical and mixing features of the reburning process and can be used for process optimization. The modeling approach is limited to combustion facilities in which radial distributions of temperature and species are relatively uniform, but in principle can be applied to more complex conditions provided adequate reactor characterization is available. The resulting model can provide powerful capabilities for the design and analysis of reburning installations.

Acknowledgments

The authors acknowledge Peter Maly and Loc Ho for conducting reburning experiments. This research was supported by the U.S. Department of Energy under Contract No. DE-AC22-95PC95251.

References

1. Kilpinen, P., Glarborg, P., and Hupa, M., *Ind. Eng. Chem. Res.* 31:1447 (1992).
2. Liu, H., Luan, T., Gibbs, B.M., and Hampartsoumian, E., *3d Asia-Pacific International Symposium on Combustion and Energy Utilization*, Hong-Kong, p. 109, 1995.
3. Cha, C.M., Kramlich, J.C., and Kosály, G., *Proc. Combust. Inst.* 27: 1427 (1999).
4. Han, D., Mungal, M., Zamansky, V., and Tyson, T., *Combust. Flame* 119:483 (1999).
5. Zamansky, V.M. and Lissianski, V.V., *Israel Journal of Chemistry* 39:63 (1999).
6. Zamansky, V.M., Sheldon, M.S., and Maly, P.M., *Proc. Combust. Inst.* 27: 3001 (1999).
7. Payne, R. and Moyeda, D., *Scale Up and Modeling of Gas Reburning*, in *FACT Vol. 18, Combustion Modeling, Scaling and Air Toxins* (A.K. Gupa, A. Moussa, C. Presser, M.J. Rini, R. Weber, and G. Woodward, eds.), The American Society of Mechanical Engineers, 1994.
8. Luan, T., Liu, H., Gibbs, B.M., and Hampartsoumian, E., *The 9th International Symposium on Transport Phenomena in Thermal-Fluids Engineering*, p. 268, 1996.
9. Rota, R., Bonini, F., Servida, A., Morbidelli, M., and Carra, S., *Combust. Sci. and Tech.* 123:83 (1997).
10. Alzueta, M.U., Bilbao, R., Millera, A., Glarborg, P., Østberg, M., and Dam-Johansen, K., *Energy & Fuels* 12:329 (1998).
11. Sheldon, M.S, Tyson, T.J., and Cole, J.A., *Spring Meeting of the Western States Section of The Combustion Institute,* Paper 97S-059, 1997.
12. Li, B.W., Moyeda, D., and Payne, R., *Proceedings of the 20th International Technical Conference on Coal Utilization & Fuel Systems*, Clearwater, Fl, p. 323, 1995.
13. Wu, K.T., Payne, R., and Nguyen, Q.H., *International Power Generation Conference*, ASME, 1991.

14. Xu, H.J,. *PhD Dissertation*, Department of Chemical Engineering, the Brigham Young University, Provo, Utah, 1999.

15. Xu, H., Smoot, L.D. and Hill, S.C., *Energy & Fuels* 13:411 (1999).

16. Dahm, W.J.A., Tryggvason, G., Frederiksen, R.D., and Stock, M.J., Local Integral Moment (LIM) Simulations, in *Computational Fluid Dynamics in Industrial Combustion* (C.E. Baukal, ed.), CRC Press, 200, p. 161.

17. Lissianski, V.V., Zamansky, V.M., and Gardiner, W.C., Combustion Chemistry Modeling, in *Gas-Phase Combustion Chemistry* (W.C. Gardiner, Jr. ed.), Springer, New York, 1999, p.1.

18. Dean, M. and Bozzelli, J.W., Combustion Chemistry of Nitrogen, in *Gas-Phase Combustion Chemistry* (W.C. Gardiner, Jr. ed.), Springer, New York, 1999, p.125.

19. Zamansky, V.M., Ho, l., Maly, P.M., and Seeker, W.R., *Proc. Combust. Inst.* 26: 2075 (1996).

20. Zamansky, V.M., Sheldon, M.S., and Maly, P.M., *Proc. Combust. Inst.* 27: 2001 (1999).

21. Lutz, A.E., Kee, R.J., and Miller, J.A., *SENKIN: A Fortran Program for Predicting Gas Phase Chemical Kinetics with Sensitivity Analysis*, Sandia National Laboratories, *Report SAND87-8248*, 1987.

22. Zwietering, T.N., *Chem. Eng. Scie.* 11:1 (1959).

23. Slaughter, D.M., Chen, S.L., Seeker, W.R., and Pershing, D.W., *Proc. Combust. Inst.* 22:1155 (1988).

24. Chen, S.L., McCarthy, J.M., Clark, W.D., Heap, M.P., Seeker, W.R., and Pershing, D.W., *Proc. Combust. Inst.* 21:1159 (1986).

25. Kolb, T., Jansohn, P., and Leuckel, W., *Proc. Combust. Inst.* 22:1193 (1988).

26. Wendt, J.O.L and Mereb, J.B., Nitrogen Oxide Abatement by Distributed Fuel Addition, *FETC Quarterly Report No. 13*, Contract DE-AC22-87PC79850, 1991.

27. Mereb, J.B. and Wendt, J.O.L., *Proc. Combust. Inst.* 23:1271 (1990).

28. Glarborg, P., Alzueta, M.U., Dam-Johansen, K., and Miller, J.A., *Combust. Flame* 115:1 (1998).

29. Kau, C. J., Heap, M. P., Seeker, W. R., and Tyson, T. J., Fundamental Combustion Research Applied to Pollution Formation. *U.S. Environmental Protection Agency Report No. EPA-6000/7-87-027, Volume IV: Engineering Analysis,* 1987.

30. Cetegen, B. M., Johnson, T. R.; Payne, R., Moyeda, D. K., and Sheldon, M. S. Effective Mixing Processes for SO_x, Sorbent, and Coal Combustion Products, *U.S. Environmental Protection Agency Report No. EPA/600/7-87/013*, 1986.

31. FLUENT, *Fluent 5 User's Guide,* Fluent, Inc., Lebanon, NH, 1998.

Table 1. Reburning parameters.

Facility	Temperature of Reburning Fuel Injection (K)	Temperature of OFA Injection (K)	$[NO_x]_i$ (ppm)
CTT	1630	1400	600
BSF	1670	1422	400-1000
TF	1800	1650	200

Table 2. Mixing parameters in CTT, BSF and TF.

Combustion facility	Mixing time in the reburning zone (ms)	Mixing time in the burnout zone (ms)	Model used to estimate mixing parameters
CTT	100	100	Single-jet-in-cross-flow
BSF	120	120	Single-jet-in-cross-flow
TF	80	120	CFD modeling

Figure Captions

Figure 1. Schematic diagrams of experimental facilities: (a) Controlled Temperature Tower (CTT), (b) Boiler Simulator Facility (BSF) and (c) Tower Furnace (TF).

Figure 2. Axial temperature profiles measured in CTT, BSF and TF. Elapsed time corresponds to the time after injection of the reburning fuel.

Figure 3. Modeling flow configuration in the reburning zone of BSF.

Figure 4. Performance of basic reburning in CTT (a), BSF (b) and TF (c). Lines represent calculations, symbols experimental data.

Figure 5. Predicted effect of mixing time on NO_x reduction for typical BSF conditions. Amount of the reburning fuel is 15% of total fuel, $[NO_x]_i$ = 600 ppm.

Figure 6. Comparison of modeling predictions (lines) with experimental data (symbols) of *Kolb et al.* [25]. Squares and dashed line correspond to the high momentum jet, filled circles and solid line to the low momentum jet. Flue gas temperature in the reburning zone is 1600 K.

Figure 7. Effect of the reburning zone stoichiometry on efficiency of the reburning process. Symbols represent measurements [26], line – model predictions. SR_1 = 1.23, $[NO_x]_i$ = 1,070 ppm.

Figure 8. Comparison of modeling predictions of NO_x concentration in the reburning zone with experimental data of *Mereb and Wendt* [26]: (a) SR_2 = 0.80, $[NO_x]_i$ = 1,140 ppm; (b) SR_2 = 0.68, $[NO_x]_i$ = 840 ppm.

Figures

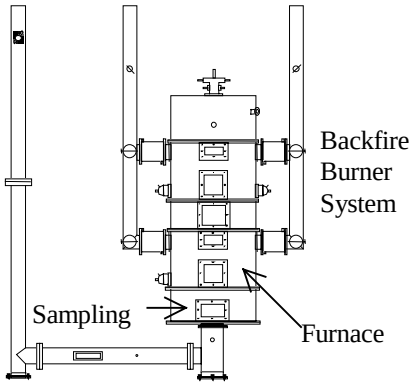

a

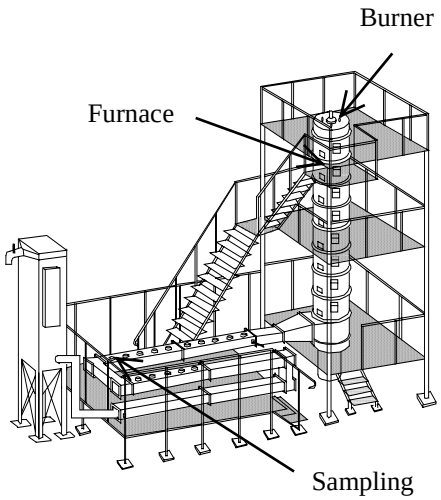

b

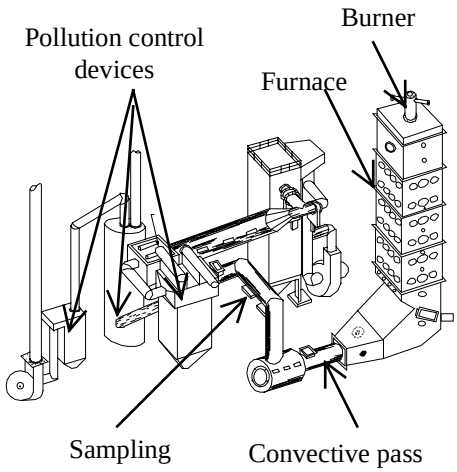

c

Figure 1.

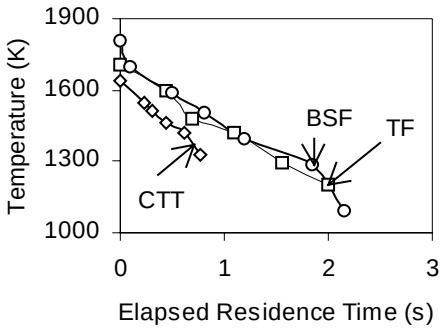

Figure 2.

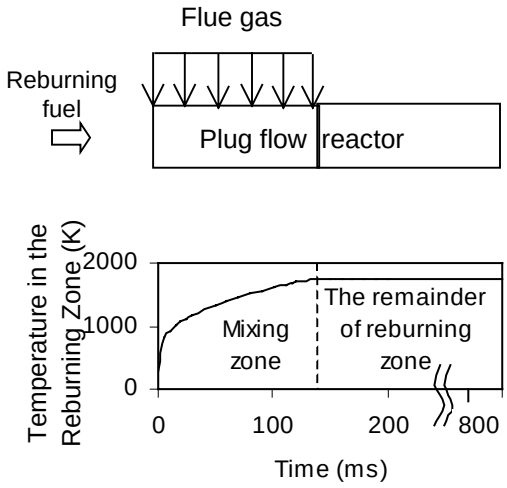

Figure 3.

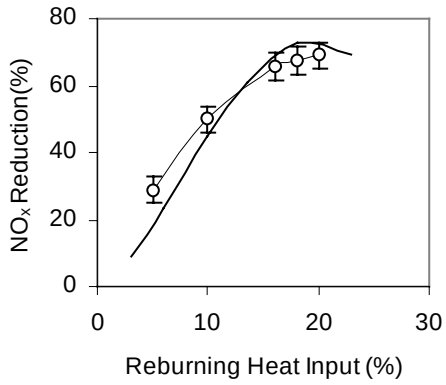
80
60
40
20
0
0
10
20
30
NOx Reduction(%)
Reburning Heat Input (%)

a

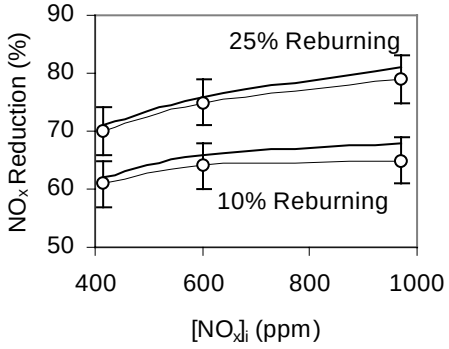
90
80
70
60
50
400
600
800
1000
25% Reburning
10% Reburning
NOx Reduction (%)
[NOx]i (ppm)

b

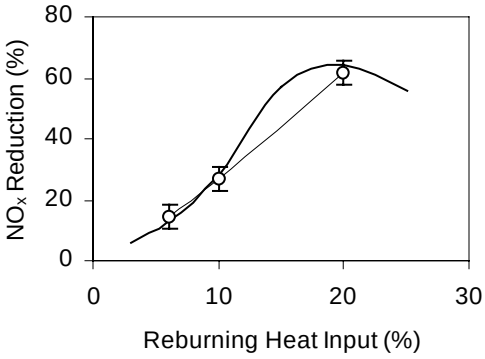
80
60
40
20
0
0
10
20
30
NOx Reduction (%)
Reburning Heat Input (%)

c

Figure 4

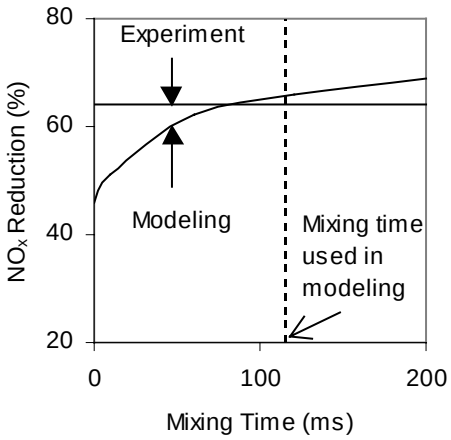

Figure 5.

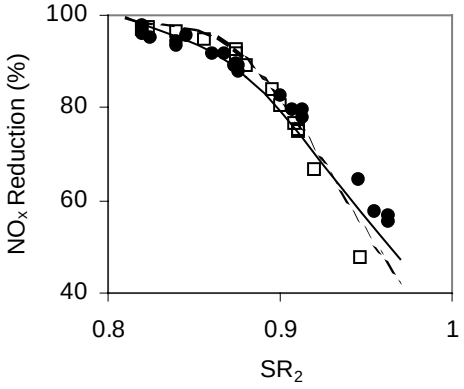

Figure 6.

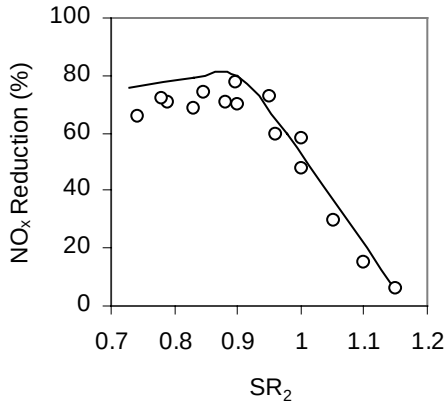

Figure 7.

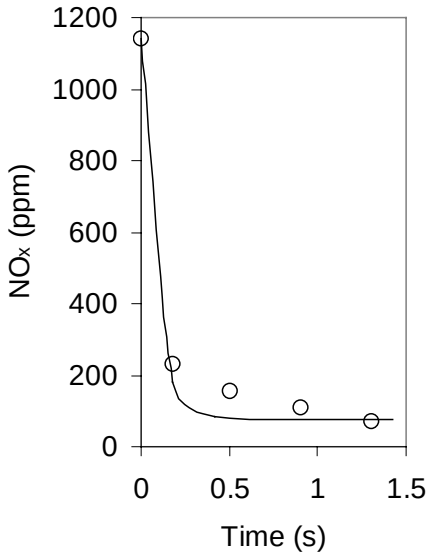
1200
1000
800
600
400
200
0
NOx (ppm)
0
0.5
1
1.5
Time (s)

a

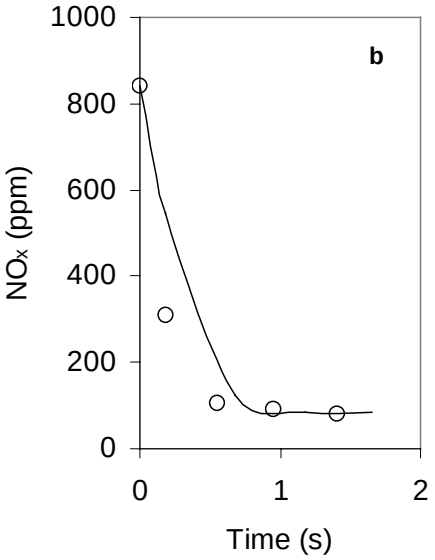
b
1000
800
600
400
200
0
NOx (ppm)
0
1
2
Time (s)

b

Figure 8.

Attachment B

Effect of Metal-Containing Additives on NO_x Reduction in Combustion and Reburning

Vitali V. Lissianski, Vladimir M. Zamansky and Peter M. Maly

GE Energy and Environmental Research Corporation

18 Mason, Irvine, CA 92618

Full-length paper

Corresponding author:

Vitali Lissianski

GE Energy and Environmental Research Corporation, 18 Mason, Irvine, CA 92618

Phone: (949) 859-8851

Fax: (949) 859-3194

E-mail: vitali.lissianski@ps.ge.com

Effect of Metal-Containing Additives on NO_x Reduction in Combustion and Reburning

Abstract

This paper describes experimental and modeling studies on the effect of metal-containing compounds on NO_x reduction. Sodium and potassium carbonates, calcium acetate, and fly ash were injected into a 300 kW combustor in one of the following configurations: with the main fuel, with the reburning fuel, or into the reburning zone. Natural gas was used as the main fuel and reburning fuel. Tests showed that co-injection of Na-, K-, and Ca-containing compounds with the main fuel reduced NO_x emissions with and without reburning. Co-injection of Na, K and Ca-containing additives along with the reburning fuel and into the reburning zone downstream of the reburning fuel had a smaller effect than co-injection with the main fuel. Fly ash showed a minimal effect on NO_x reduction. A potential benefit of using calcium-containing additives in reburning is reduced SO_2 emission during coal combustion. About 50% SO_2 reduction was achieved with injection of 1,000 ppm of $Ca(OH)_2$ with the main fuel.

Modeling was used to determine the mechanism of the effect of Na-containing additives on NO_x reduction. The model combined a detailed description of the reburning chemistry with a simplified representation of mixing. Modeling suggested that reduction of NO_x emissions in the presence of sodium-containing compounds was due to the inhibition of the combustion process by sodium. Since NO_x formation via thermal and fuel-NO mechanisms strongly depend on the local combustion environment, NO_x formation in the main combustion zone was inhibited because H, OH and O concentrations in the combustion zone in the presence of Na decreased. The increase in NO_x reduction in the reburning zone was due to slower oxidation of the reburning fuel in the presence of Na.

Effect of Metal-Containing Additives on NO_x Reduction in Combustion and Reburning

Vitali V. Lissianski, Vladimir M. Zamansky and Peter M. Maly

GE Energy and Environmental Research Corporation (GE EER)

18 Mason, Irvine, CA 92618, USA

Introduction

A number of technologies utilize injection of additives for the selective reduction of NO in high temperature flue gas [1-3]. Different variants of reburning and N-agent injection (Advanced Reburning [4-7]) are capable of achieving 90%+ NO_x reduction and can reduce NO_x emissions from coal-fired boilers and furnaces below about 130 ppm – the regulatory level recently established by the U.S. EPA for a 22 State region in the Northeast of the United States. In Advanced Reburning, the additives (N-agent – for example, urea or ammonia – alone or with promoters) are injected in one or several locations: reburning and burnout zones, or downstream of the burnout zone. The promoters are water-soluble inorganic salts (for example, Na_2CO_3 and $NaHCO_3$) that can be added to aqueous N-agents. It was suggested [6,7] that Na-containing compounds increased the radicals pool via chain reactions $Na + H_2O \rightarrow NaOH + H$ and $NaOH + M \rightarrow Na + OH + M$ when injected at the end of the reburning zone and thus increased the activity of N-agent in removing NO_x.

Recent experimental data [8] show that levels of NO_x reduction comparative to Advanced Reburning can be achieved by injection of iron-containing compounds without injecting N-agent into combustion and reburning zones. Injection of iron compounds has an advantage over some Advanced Reburning configurations since it does not require a separate injector for the additive: the additive can be co-injected with main or reburning fuels. An increase in ash loading as a

result of additive injection is not significant relative to inherent ash loading in combustion of solid fuels. The experimental data [8] show that the efficiency of iron-containing compounds depends on location of the additive injection and on the nature of the compound. While the mechanism of NO_x reduction by iron-containing compounds is under investigation, there is a possibility that other metal-containing compounds are also effective promoters of NO_x reduction. Mechanism of their effect on NO_x reduction may be different from that suggested [6,7] for Advanced Reburning since N-agent is not injected in this case.

This paper describes experimental studies on the effect of several metal-containing compounds on NO_x reduction in a pilot-scale combustion facility. Experimental data show that under certain conditions, addition of small amounts of sodium-, potassium- and calcium-containing compounds can substantially increase the efficiency of NO_x reduction in combustion and reburning processes. Modeling of the effect of sodium on reactions in the main combustion and reburning zones is also presented.

Experiment

Experimental Setup

A series of pilot-scale tests was conducted in a 300 kW Boiler Simulator Facility (BSF) to characterize the effect of additives on reburning. The BSF (Fig. 1a) is designed to provide an accurate sub-scale simulation of the flue gas temperatures and composition found in a full-scale boiler, and is described elsewhere [9]. It consists of a burner, vertically down–fired radiant furnace (0.55 m ID, 7 m height), and horizontal convective pass. There are no recirculation zones in the furnace or convective pass. The convective pass is refractory lined and has dimensions of 0.2 m by 0.2 m. Reburning fuel and OFA were injected through L-shaped radial injectors, aligned on the centerline of the furnace. They were oriented upward. The injectors did not have

swirl vanes. A variable swirl diffusion burner with an axial fuel injector is used to simulate the approximate temperature and gas composition of a commercial burner in a full-scale boiler. Gas temperature profiles were measured using a suction pyrometer axially along the furnace. The furnace was also traversed radially at each sample location. The BSF temperature profile is shown in Fig. 1b. The temperature gradient in the BSF in the range of 1200-1700 K was about –300 K/s. In the main combustion zone primary air is injected axially, while the secondary air stream is injected radially through the swirl vanes to provide controlled fuel/air mixing. Numerous ports located along the axis of the facility allow supplementary equipment such as reburning injectors, additive injectors, overfire air injectors, and sampling probes to be placed in the furnace.

A continuous emissions monitoring system (CEMS) was used for on-line analysis of flue gas composition. The CEMS consisted of a heated sample line, sample conditioning system (to remove moister and particulate), and gas analyzers. Sampling was performed in the convective pass at a gas temperature of 700 K. The sample probe was placed on the centerline of the convective pass. NO_x, CO, and SO_2 were measured at a precision of 1 ppm. O_2 and CO_2 were measured at a precision of 0.1%. Previous studies have indicated that CEMS data are affected minimally by interfering species.

Effect of Metals on NO_x Reduction

Previous experimental data [6,7] demonstrated that alkali compounds reduce NO_x concentrations when co-injected with N-agent into the reburning zone (Advanced Reburning). It is worthwhile to determine if the same and other metal-containing additives can affect the reburning process when injected alone. Sodium and potassium carbonates, and calcium acetate were selected for tests and were injected into BSF as aqueous solutions in one of the following configurations: with the main fuel, with the reburning fuel or into the reburning zone

downstream of the reburning fuel injection. Solutions were injected by atomizing them with a twin-fluid nozzle. For comparison, experiments also were conducted with fly ash generated by coal combustion and containing compounds of the same metals. Dry powdered ash was added by pneumatically transporting it to the furnace and injecting through an axial injector. In all tests natural gas was used as main and reburning fuels. The amount of the reburning fuel was 18% of the total heat input. The reburning fuel was injected at 1670 K and overfire air (OFA) was injected at 1300 K. Injection of additives into reburning zone downstream of the reburning fuel was performed at a flue gas temperature of 1590 K. Tests showed that injection of equivalent amount of water without metal-containing compounds did not affect temperature profile in BSF and had no effect on NO_x. The initial NO_x concentration was set at 600 ppm by adding ammonia to the combustion air. The stoichiometric ratio (SR) in the main combustion zone was 1.15, and the amount of OFA was such that SR in the burnout zone (including previously added fuel) was 1.15.

Figure 2 shows the effect of Na, K and Ca compounds co-injected with the main fuel in the presence and in the absence of reburning. Injection of metal-containing compounds in the absence of reburning ("metal only" bars) resulted in 16%-21% NO_x reduction. Reburning itself provided 66% NO_x reduction. Injection of 100 ppm metal compounds (of total flue gas) with the main fuel in the presence of reburning provided an additional 4-7 percentage points of NO_x reduction. The amount of metal in flue gas is calculated assuming that all metal is in vapor phase. Results presented in Fig. 2 illustrate that sodium- and potassium-containing additives are slightly more effective than calcium-containing compounds when added with the main fuel.

Figure 3 shows the effect of promoter concentration on NO_x reduction. In the absence of reburning, the effect of the additive first increases as concentration of additive increases and then decreases. Up to approximately 28% NO_x reduction was achieved at 500 ppm of Na or K in the flue

gas. The additives also improved the efficiency of reburning by 11 percentage points. The effect of additives on reburning also first increases and then slightly decreases (although not as significantly as in the absence of reburning). Both Na and K show similar effects on NO_x reduction.

Figure 4 demonstrates that similar results were obtained by injecting sodium along with the reburning fuel. Injection of sodium carbonate improves NO_x control efficiency by up to 6 percentage points. This effect is slightly smaller than that observed for Na injection with the main fuel and is about 15% smaller than the effect observed for Fe compounds [8].

Figure 5 demonstrates the effects of Na and Ca injection into reburning zone downstream of the reburning fuel. NO_x reduction in this case is less than that for the injection with main and reburning fuels. Injection of sodium carbonate reduces NO_x concentration by additional 4 percentage points, while calcium acetate reduces NO_x by 3 percentage points.

Figure 6 shows the effect of sodium carbonate injection on CO emissions. The baseline corresponds to the level of CO in flue gas in the absence of reburning and additives. Reburning increases CO emissions by about 20%. The "Na only" bar corresponds to the injection of additive with the main fuel in the absence of reburning. CO emissions appear to slightly increase during Na injection, most notably for the no-reburning case.

Effect of Fly Ash on NO_x Reduction

It is known that coals, chars and fly ash produced by coal combustion contain mineral compounds, including Na, K, Ca, Fe, and other metals that may become volatile at combustion temperatures and affect NO_x concentration. For example, the presence of CaO in char has been shown [10-12] to increase reaction rate of NO with char. Catalytic decomposition of NO on various metallic oxides has been reported by Winter [13].

The amount of metals in fly ash varies and depends on the coal type. Table 1 shows composition of fly ash used in current tests. It was generated from several coal sources, most

notably Knott-Floyd Land which is a Kentucky coal. The iron content in fly ash is high (14.95%). It also has significant calcium oxide and potassium oxide content, 3.00% and 2.65% respectively. Figure 7 shows the effect of fly ash injected along with the reburning fuel. Fly ash was tested in two forms: calcinated at 1200 K, and calcinated/ground/hydrated. Both forms of fly ash showed minimal effect on NO_x reduction. However, grinding and hydrating slightly improve the efficiency of fly ash, probably by increasing surface area.

One can note that the metal additives are much more effective than the compounds of the same metals present in fly ash. The flow rate of fly ash injection in tests was such that concentrations of iron, calcium, potassium and sodium from fly ash in flue gas (if all metals were released in atomic form) would be approximately 400 ppm, 90 ppm, 120 ppm, and 60 ppm respectively. However, their effect on NO_x reduction is, as shown in Figure 7, only 1-2 percentage points. The negligible effect of these metals can be explained by the difference in the chemical nature of metal compounds in the additives versus fly ash. Although traditional ash analyses present mineral composition in the form of metal oxides, the oxides are not the actual forms of metals in fly ash. The metals are mainly present in the form of sulfides and silicate-alumosilicate matrixes which are more stable than carbonates and acetates at high temperatures and, thus, are not effective in reactions with combustion radicals and have minimal effect on NO_x reduction.

Effect of Ca on SO_2 Emissions

Tests showed that calcium-containing compounds were less effective than alkali metals in reduction of NO_x emissions. However, calcium has an advantage over alkali metals since it does not contribute to deposition on heat transfer surfaces and thus may be preferred in

commercial applications. Other potential benefit of using calcium-containing compounds is reduced sulfur emissions from coal combustion. To determine the efficiency of NO_x and SO_2 reduction during coal combustion, tests were conducted with Utah coal as the main fuel. The initial amount of SO_2 generated by coal combustion was 800 ppm. The reburning fuel was natural gas.

Figures 8 and 9 show effects of $Ca(OH)_2$ co-injection with main and reburning fuel on NO_x and SO_2 emissions. While the efficiency of NO_x reduction does not depend significantly on the method of additive injection, the efficiency of SO_2 reduction is much higher when the additive is injected with the main fuel (about 50%).

Summary of Experimental Data

The following conclusions can be drawn from experimental data.

- Sodium and potassium are more effective promoters of NO_x reduction than calcium. Addition of alkali-containing compounds in the reburning zone results in an increase of NO_x reduction by up to 11 percentage points. Alkali-containing compounds are less effective than iron-containing compounds, which were found [8] to reduce NO_x in the reburning zone by up to 20 additional percentage points.
- The promoters are most effective when injected with main or reburning fuel. Injection into the reburning zone is less effective.
- The form in which promoters are injected is important. Tests with fly ash suggest that metal sulfides and alumosilicates are not effective promoters of NO_x reduction.
- The effect of alkali metals injection on NO_x reduction is less than the combined effect of N-agent and metal injection [6,7] into the reburning zone, which for similar experimental conditions can achieve over 90% NO_x reduction.

- Injection of Ca-containing compounds reduced both NO_x and SO_2 emissions.

Model Setup

Kinetic modeling helps to understand the mechanism of the effect of additives on NO_x reduction. A previously developed model [14] of the reburning process was modified to describe injection of metal-containing additive with main fuel, along with reburning fuel and into reburning zone. The model combined a detailed description of the reburning chemistry with simplified representation of mixing and utilized well-stirred and plug-flow reactors to describe processes that occur in the boiler: combustion in the main combustion zone, mixing of the reburning fuel with flue gas, NO_x reduction in the reburning zone, addition of overfire air, and reactions in the burnout zone. The mixing was always described by adding flue gas to the injecting stream (inverse mixing) over mixing time. For example, mixing in the reburning zone was described by adding flue gas to the flow of natural gas; mixing of OFA was described by adding flue gas to the OFA. The model of inverse mixing was found to give good description of experimental data on basic reburning [14], Advanced Reburning [15], and Selective Non-Catalytic Reduction [16]. Mixing of the reburning fuel and OFA with flue gas occurred over a certain period of time (mixing time). Mixing times and temperature profiles in mixing regions of BSF were estimated using a single jet in cross flow model as described in [14]. The model took into account mixing and thermal BSF characteristics. The temperature gradient along the reactor was assumed to be –300 K/s. Mixing times in the reburning and burnout zones were estimated [15] to be 120 ms.

Modeling Results

Since tests showed that Na had the most significant effect on NO_x reduction in all tested configurations, and since the mechanism of Na_2CO_3 decomposition and reactions of Na-

containing species are readily available [16], modeling work was conducted to describe the injection of Na_2CO_3 additive. The kinetic model of the reburning process [17] was supplemented with 20 reactions of four Na-containing species [16].

The reduction of NO_x in the presence of Na-containing compounds can be explained by heterogeneous processes, reactions in the gas phase, or a combination of these two mechanisms. It was shown [16] that at temperatures higher than 1000 K Na_2CO_3 in the presence of water quickly decomposes to form NaOH(g) and CO_2. Thermodynamic calculations conducted with utilization of code presented in [18] also suggest that at temperatures relevant to the reburning process most Na is present in the gas-phase in the form of NaOH(g) (about 90% of the total Na) and in the atomic form Na(g). Thus, it is unlikely that any solid Na-containing species are present in a significant amount in flue gas at reburning conditions. Based on previous results [16] and thermodynamic calculations, it was assumed in modeling that the homogeneous mechanism of NO_x reduction by Na-containing species was dominant.

Effect of Na on NO_x Reduction in the Main Combustion Zone

Experiments demonstrated that injection of Na with the main fuel in the absence of reburning reduced NO_x emissions by about 20%. Combustion in the main combustion zone is a complex process which is strongly affected by gas dynamic processes within combustion chamber. However, chemistry aspects of the effect of Na on NO_x formation and destruction in flame can be understood by isolating mixing effects from chemical kinetics. The main combustion zone in modeling was represented by a well-stirred reactor. The mixture entering the reactor corresponded to the methane–air mixture with SR = 1.15. It is known that the composition of products coming from well-stirred reactor depends on the reactor residence time. Thus, results of modeling are sensitive to the residence time. The residence time adopted in the model for the main combustion zone was 10 ms. Based on flame observations in the BSF main

combustion zone, this time is believed to be representative of the residence time in the flame. While uncertainty in the value of the residence time in modeling affects the absolute value of the effect of Na on NO_x reduction, the chemical mechanism of the effect stays the same.

Modeling suggests that the effect of sodium additives on NO_x concentration in the main combustion zone can be explained as follows. Modeling predicts that addition of sodium carbonate into the main combustion zone results in its fast decomposition and reaction with water to form sodium hydroxide, NaOH, CO_2 and sodium atoms. It is known [19] that sodium-containing compounds are strong inhibitors of the combustion process. The suppression of flame occurs through the sequence of reactions in which active species are removed. Modeling [20] suggested that the removal of radicals in flames could occur through the following chain reaction

$$NaOH+H \rightarrow Na+H_2O \quad (1)$$

$$Na+O_2+M \rightarrow NaO_2+M \quad (2)$$

$$NaO_2+OH \rightarrow NaOH+O_2 \quad (3)$$

The net action of sodium species in reactions (1)-(3) is equivalent to the conversion of H atoms and OH radicals into H_2O

$$\text{Net:} \quad H+OH \rightarrow H_2O \quad (4)$$

Modeling predicts that concentrations of active species in the combustion zone decrease as a result of Na addition with the main fuel. For example, concentrations of oxygen and hydrogen atoms decrease in the presence of 100 ppm Na by 40% and 50% respectively. Since NO_x formation via thermal and fuel-NO mechanisms strongly depend on the local combustion environment, reduction in concentrations of major radicals results in decrease of NO_x concentration. Figure 10 shows a comparison between modeling predictions and experimental data for Na injection into the main combustion zone without reburning (“Na only” bars). Overpredicting the efficiency of NO_x reduction can be caused by several factors. The first factor

is that well-stirred reactor does not give an exact representation of the main combustion zone. Particularly, combustion in the main combustion zone is unmixed, while in the model fuel and air are assumed premixed. Effect of turbulence on NO_x formation is also not taken into account in the model. The second factor is that the residence time in the reactor can be different from 10 ms adopted in the model.

Effect of Na on NO_x Reduction in the Reburning Zone

The effect of Na on NO_x reduction for the reburning configuration when additive is injected with the main fuel in the presence of reburning can be divided into two parts. First, Na reduces NO_x formation in the main combustion zone via the mechanism described in previous section. Second, Na reduces NO_x emissions in the reburning zone by affecting reburning chemistry. All three configurations used in tests (injection with main and reburning fuels, and into reburning zone) were considered in modeling.

Modeling suggests that sodium additives decrease NO_x concentration in the reburning zone by decreasing oxidation rate of the reburning fuel. The presence of sodium results in a decrease in radical concentrations during the reburning process. It was observed in modeling that the reburning fuel is oxidized during the early part of the reaction with and without sodium addition. However, in the presence of sodium, the fuel is oxidized over a longer period of time. Fuel oxidation generates hydrocarbon-containing radicals which reduce NO to N_2. At the same time, the hydrocarbon radicals react with other non-carbon atoms and radicals (H, OH, O etc.) and are transformed into other products. In the presence of sodium, the concentration of non-carbon radicals is smaller, reaction rates of hydrocarbon radicals with non-carbon radicals decrease which results in a higher rate of the reaction of hydrocarbon radicals with NO. Thus, modeling suggests that the effect of sodium addition can be explained by the removal of non-carbon radicals by sodium species via reactions (1-3).

Additive co-injection with reburning fuel is more effective than injection into reburning zone downstream of the reburning fuel because in the latter case by the time the additive evaporates and mixes with flue gas most reburning fuel has been oxidized and most NO_x reduction in the reburning zone has already occurred.

It was suggested previously [6,7] that the effect of Na-containing compounds on NO_x reduction for *co-injection of promoter and N-agent* at the end of the reburning zone can be explained by the ability of Na to increase mixture reactivity by producing radicals in the chain reactions (1) – (3). Thus, mechanism of NO_x reduction by Na depends on the presence or absence of N-agent and location of Na injection, and is quite different for these two cases. These mechanisms do not contradict but rather complement each other and demonstrate a unique ability of Na to act as an inhibitor or as a promoter of a combustion system depending on the system reactivity. If radical concentrations in the combustion system are high (main combustion zone and initial part of the reburning zone where injection, mixing and oxidation of the reburning fuel occurs), Na atoms inhibit the combustion system by reducing H and OH concentrations via reactions (1) – (3). However, if radical concentrations are low (end of the reburning zone), Na atoms increase the concentrations of H and OH via reverse reactions (1) – (3).

Figure 10 compares experimental data and modeling predictions on the effect of sodium injection both along with the reburning fuel and into reburning zone downstream of reburning fuel on NO_x reduction. Modeling results demonstrate good agreement with experimental data for both locations of additive injection. Both modeling and experimental data suggest that the additive is most effective when added with the main fuel, whereas the addition along with the reburning fuel is slightly less effective. Injection of Na with the main fuel is the most effective because in this case the additive reduces NO_x concentration both in the main and reburning zones.

Effect of Na on CO Emissions

Modeling also qualitatively explains experimental results on increasing CO emissions in the presence of Na additives. Modeling predicts that fuel oxidation in the reburning zone generates a significant amount of CO. For 18% reburning heat input, the concentration of CO at the end of the reburning zone is about 2.2%. The CO formed in the reburning zone is oxidized to CO_2 when OFA is injected to complete combustion. The temperature of OFA injection should be high enough to provide complete CO oxidation. Since Na acts as an inhibitor of the combustion process, it decreases concentrations of active species in the burnout zone, including H atoms and OH radicals. Reaction (1) has the largest effect on the rate of CO oxidation among reactions of Na-containing species. This reaction inhibits the oxidation process by removing H atoms which otherwise would react with O_2 via

$$H + O_2 \rightarrow OH + O. \qquad (5)$$

Since CO oxidation mainly occurs in the reaction with OH radicals

$$CO + OH \rightarrow CO_2 + H \qquad (6)$$

which are mostly formed in reaction (5), reaction (1) slows down the CO oxidation resulting in higher CO emissions.

Quantitative description of experimental results on CO emissions is difficult within the framework of the adopted model since it does not take into account non-uniformity of temperature distribution in the BSF. Non-homogeneity of the temperature field in the burnout zone and incompleteness of mixing are main reasons of CO emissions in tests even without additives. To avoid high CO concentrations in flue gas, OFA has to be added at temperatures higher than 1300 K.

Conclusions

The current work demonstrates that small addition rates of Na-, K- and Ca-containing compounds increase the efficiency of NO_x control in combustion and reburning. Utilization of Ca-containing compounds also results in reduction of SO_2 emissions. Additives of Na and K are more effective in NO_x reduction than additives of Ca. Comparison of relative effects of alkali- and iron-containing compounds on NO_x reduction shows that iron-containing compounds are significantly more effective. Kinetic modeling was conducted to explain the experimentally observed effects of Na-containing compounds on NO_x reduction. While contribution of heterogeneous reactions to NO_x reduction in the presence of Na-containing additives can not be eliminated, the thermodynamic data suggest that Na at the reburning conditions are present in the gas-phase. This makes the suggested homogeneous mechanism the most likely explanation of the effect of Na on NO_x reduction. Na-containing additives remove active combustion species (H and OH) via chain reaction and, thus, reduce the rate of NO formation in the main combustion zone. The increase in NO_x reduction in the reburning zone is due to slower oxidation of the reburning fuel in the presence of Na. This mechanism is different from that previously suggested [6,7] to explain the effect of Na co-injection with N-agent at the end of the reburning zone on NO_x reduction and is a reflection of the unique ability of Na to increase or decrease concentrations of active species in the combustion system depending on its reactivity. The higher efficiencies of Na- and K-containing compounds than Ca-containing compounds in reduction of NO_x emissions can be explained by higher efficiency of alkali compounds in suppression of combustion as observed in flame tests [19].

Acknowledgment

This research was supported by the U.S. Department of Energy under Contract No. DE-AC22-95PC95251 (Project Manager is Thomas J. Feeley).

Bibliography

1. Lyon, R.K., *U.S. Patent 3,900,554* (1975).
2. Arand, J.K., Muzio, L.J. and Sotter, J.G., *U.S. Patent 4,208,386* (1980).
3. Schrecebgost, R.A., Gomez, A.F., Pratapas, J.M., Johnson, R.A. Demonstration of Amine Enhanced Fuel Lean Gas Reburn at Public Service Electric & Gas Mercer Station, *Presented at the 1998 Spring ASME-Ice Division Engine Technology Conference*, Florida, 1998.
4. Chen, S.L., Lyon, R.K. and Seeker, W.R., *Environ. Progress* 10:182 (1991).
5. Zamansky, V.M., Maly, P.M. and Seeker, W.R., *U.S. Patent 5,756,059* (1998).
6. Zamansky, V.M., Ho, l., Maly, P.M. and Seeker, W.R., *Proc. Combust. Inst.* 26:2075 (1996).
7. Zamansky, V.M., Sheldon, M.S. and Maly, P.M., *Proc. Combust. Inst.* 27:2001 (1999).
8. Zamansky, V.M., Maly, P.M., Cole, J.A., Lissianski, V.V. and Seeker, W.C., Metal-Containing Additives for Efficient NO_x Control, *U.S. Patent Application*, 2000 (Patent No. will be provided before publication).
9. Slaughter, D.M., Chen, S.L., Seeker, W.R., and Pershing, D.W., *Proc. Combust. Inst.* 22:1155 (1988).
10. Guo, F., Hecker, W.C., *Proc. Combust. Inst.* 26:2251 (1996).
11. Chen, W.-Y., Extent of Heterogeneous Mechanisms During Reburning of Nitrogen Oxide, *Presented at the Annual Meeting of American Institute of Chemical Engineers*, Paper #78k, 1995.
12. Illán-Gómez, M.J., Linares-Solano, A., Radovic, L.R., and Salinas-Martínez de Lecea, C., *Energy Fuels* **9**, 97 (1995).
13. Winter, E.R.S., *J. of Catalysis* 22:158 (1971).
14. Zamansky, V.M. and Lissianski, V.V., *Israel Journal of Chemistry* 39:63 (1999).

15. Lissianski, V.V., Zamansky, V.M., Maly, P.M. and Sheldon, M.S., Optimization of Advanced Reburning via Modeling, *Proc. Combust. Inst.* 28 (2000).
16. Zamansky, V.M., Maly, P.M., Ho, L., Lissianski, V.V., Rusli, D., and Gardiner, W.C., *Proc. Combust. Inst.* 27:1443 (1999).
17. Glarborg, P., Alzueta, M.U., Dam-Johansen, K., and Miller, J.A., *Combust. Flame* 115:1 (1998).
18. Feitelberg, A.S. *CET93 for Windows 95/NT 4.0: A Chemical Equilibrium and Transport Properties Calculator*, General Electric Company, 1998.
19. Babushok, V., Tsang, W., Linteris, G.T., and Reinelt, D., *Combust. Flame* 115:551 (1998).
20. Schofield, K. and Steinberg, M., *J. Phys. Chem.* 96:715 (1992).

Table 1. Mineral composition of fly ash generated by combustion of a Kentucky coal.

Composition	Weight %
Silicon oxide	55.74
Aluminum oxide	18.68
Titanium dioxide	0.94
Iron oxide	14.95
Calcium oxide	3.00
Magnesium oxide	2.65
Potassium oxide	2.65
Sodium oxide	0.93
Sulfur trioxide	1.83
Phosphorus pentoxide	0.33
Barium oxide	0.16
Manganese oxide	0.01
Total	100.00

Figure Captions

Figure 1. Schematic diagram of BSF (a) and temperature profile in BSF (b).

Figure 2. Effect of metal-containing compounds injected with the main fuel on NO_x reduction. Amount of metal is 100 ppm. 1 – Na, 2 – K, 3 – Ca.

Figure 3. Na and K performance as a function of promoter concentration with (a) and without (b) reburning. Promoters are injected with the main fuel. Squires and dotted lines represent Na, triangulars and solid lines represent K. Dashed line represents basic reburning.

Figure 4. NO_x reduction as function of Na_2CO_3 and iron waste concentrations. Additives are co-injected with the reburning fuel at 25% reburning.

Figure 5. Injection of 100 ppm Na and Ca into reburning zone at 1590 K.

Figure 6. Effect of 100 ppm Na addition on CO emissions.

Figure 7. Effect of fly ash co-injection with reburning fuel on NO_x reduction. 1- Reburning, 2 – reburning + calcinated fly ash, 3 – reburning + calcinated/hydrated fly ash.

Figure 8. Calcium promoter NO_x control performance during Utah coal firing. Squires correspond to co-injection with main fuel, circles to co-injection with reburning fuel.

Figure 9. Calcium promoter SO_2 capture during Utah coal firing. Squires correspond to co-injection with main fuel, circles to co-injection with reburning fuel.

Figure 10. Comparison of modeling predictions with experimental data on the effect of Na_2CO_3 on NO_x reduction. Open bars represent experimental data, shaded bars modeling.

Figures

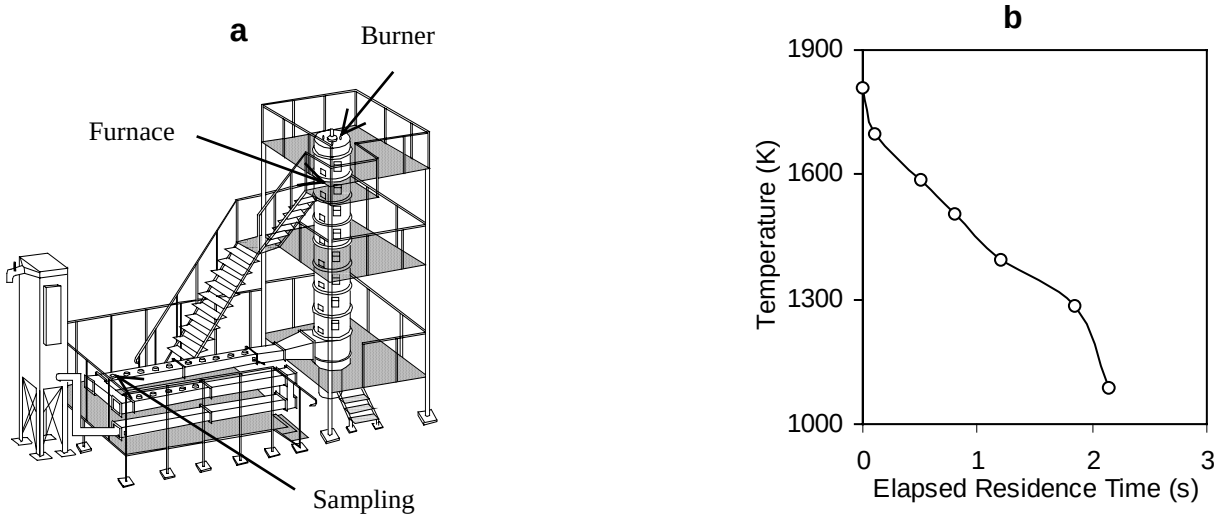

Figure 1

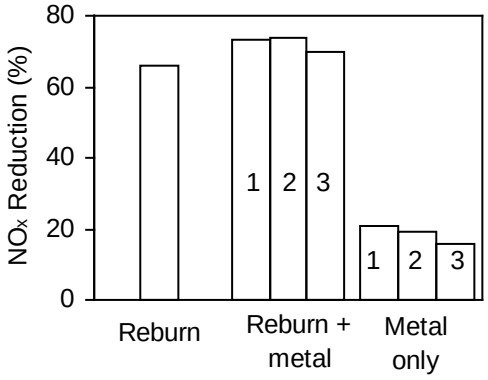

Figure 2

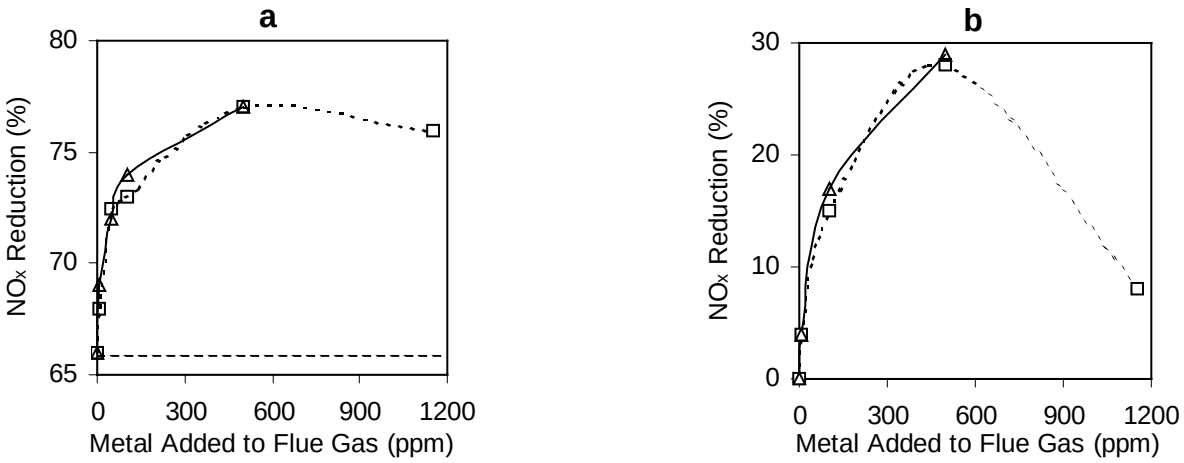

Figure 3

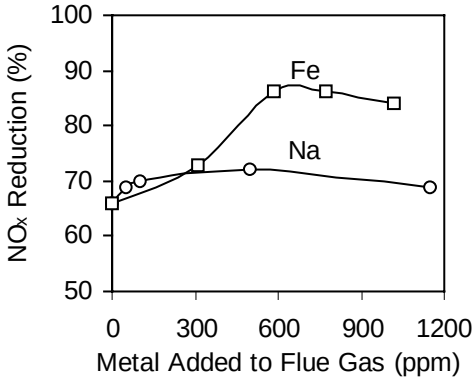

Figure 4

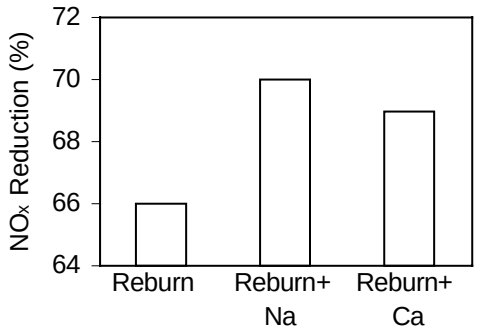

Figure 5

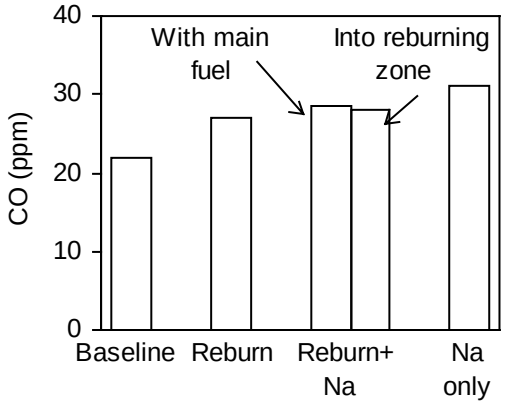

Figure 6

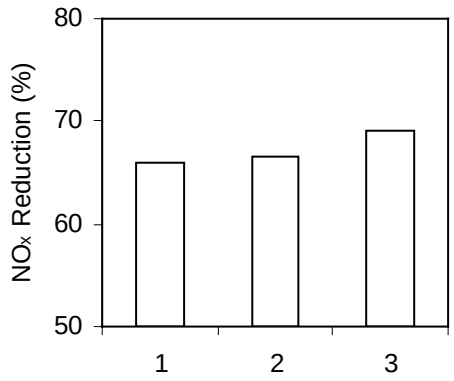

Figure 7

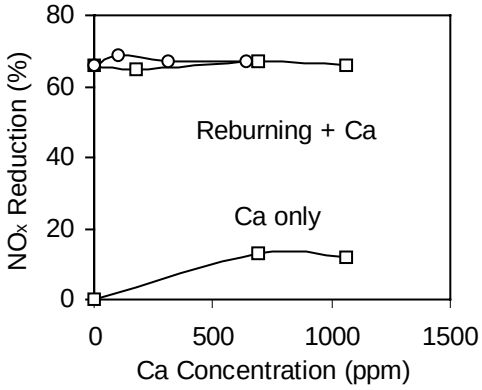

Figure 8

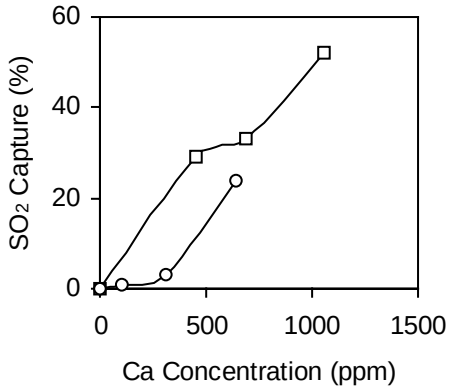

Figure 9

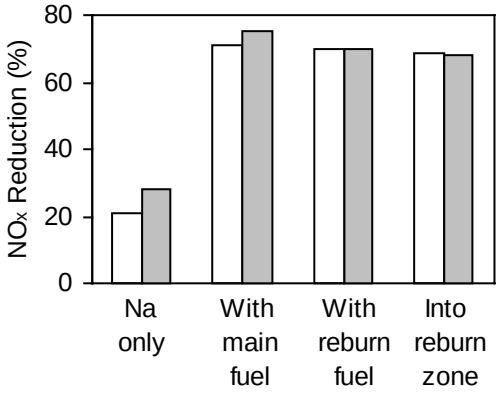

Figure 10